Spin-gap behavior and charge ordering in α'-NaV$_2$O$_5$ probed by light scattering

M. Fischer, P. Lemmens, G. Els, and G. Güntherodt

2. Physikalisches Institut, RWTH Aachen, Templergraben 55, D-52056 Aachen, Germany

E. Ya. Sherman

Moscow Institute of Physics and Technology, 141700 Dolgoprudny, Moscow region, Russia

E. Morré, C. Geibel, and F. Steglich

Max-Planck-Institut für Chemische Physik fester Stoffe, D-01187 Dresden, Germany

We present a detailed analysis of light scattering experiments performed on the quarter-filled spin ladder compound α'-NaV$_2$O$_5$ for the temperature range 5 K$\leq T \leq$300 K. This system undergoes a phase transition into a singlet ground state at $T=34$ K accompanied by the formation of a superstructure. For $T \leq 34$ K several modes were detected. Three of these modes are identified as magnetic bound states. Experimental evidence for charge ordering on the V sites is detected as an anomalous shift and splitting of a V-O vibration at 422 cm^{-1} for temperatures above 34 K. The smooth and crossoverlike onset of this ordering at $T_{CO}=80$ K is accompanied by pretransitional fluctuations both in magnetic and phononic Raman scattering. It resembles the effect of stripe order on the super structure intensities in La$_2$NiO$_{4+\delta}$. [S0163-1829(99)02434-0]

I. INTRODUCTION

Low-dimensional quantum spin systems have recently attracted strong experimental as well as theoretical interests. Despite their principally simple crystal structure they exhibit a variety of unusual ground states and excitations. One of these unusual phenomena which are very specific to one-dimensional spin systems is the spin-Peierls transition. The nature of this transition is an instability of a spin-1/2 Heisenberg chain against a dimerized ground state due to a coupling of the spins to the lattice. This instability appears as a well defined thermodynamic phase transition at a finite temperature. Thereby the lattice undergoes a distortion leading to a small structural change and thus to a super structure. On the other hand, two neighboring spins dimerize leading to a singlet ground state and a singlet-triplet gap in the magnetic excitation spectrum.[1–3]

If an additional frustration due to next nearest neighbor exchange interaction is present, as, e.g., in the inorganic spin-Peierls compound CuGeO$_3$,[4–7] a magnetic singlet bound state exists that is combined of two triplet excitations. This bound state is indeed observed in Raman experiments due to exchange light scattering (no spin flip, i.e., $\Delta S=0$).[8–10] In spin ladders multiple magnetic bound states of triplet or singlet character are expected.[11] Here, with increasing spin frustration the binding energy and the number of bound states increases. It is proposed that the quantum phase transition from a gapless into a quantum disordered state with gapped elementary excitations is characterized by the condensation of many particle bound states.[11]

Recently, it has been proposed that α'-NaV$_2$O$_5$ might be the second inorganic spin-Peierls compound with a transition temperature $T_{SP}=34$ K.[12] Indeed, susceptibility data of α'-NaV$_2$O$_5$ can be fit very well by a one-dimensional Heisenberg chain model yielding an exchange interaction of $J=480$ and 560 K determined for temperatures below and

above T_{SP}, respectively.[12,13] For $T \leq T_{SP}$ an isotropic drop in the susceptibility corresponding to the opening of a singlet-triplet gap of $\Delta_{ST}=85$ K has been observed. X-ray measurements[14] as well as Raman scattering[13] proved the existence of a super structure formation.

However, recent X-ray structure data analysis at room temperature is not in favor of the previously reported non-centrosymmetric structure[15] and of the picture of a one-dimensional Heisenberg chain. They clearly give evidence for the centrosymmetric space group (D_{2h}^{13}) leading to only one type of V site with a formal valence $+4.5$ in this compound.[16,17] The V sites then form a quarter-filled ladder running along the b axis with rungs along the crystallographic a axis. For low energy scales the quarter-filled ladder can effectively be mapped onto a $s=1/2$ chain along the b axis as there is a considerable large charge transfer gap. Both the estimated charge transfer gap and the exchange coupling J agree well with the experimental observations.[17,18] In principle, it is possible that this effective chain shows all the features one may expect from an ordinary one-dimensional spin chain, including a spin-Peierls instability.

On the other hand, for quarter-filled bands there are several other instabilities such as spin density wave or charge density wave transitions. As shown by Seo and Fukuyama[19] intersite Coulomb interaction is the most important parameter in this sense. It introduces charge disproportionation or other instabilities of the system. Therefore several scenarios for the phase transition in α'-NaV$_2$O$_5$ are discussed. One possibility is to assume a primary charge order of the V sites into V^{4+} with $s=1/2$ and V^{5+} with no spin on either leg of the ladder leading to linear spin chains in b direction. This charge ordering is followed by a secondary spin-Peierls transition.[20]

A different approach has been chosen by Mostovoy and Khomskii.[21] Starting with an electronic Hamiltonian including not only hopping terms and on-site Coulomb repulsion
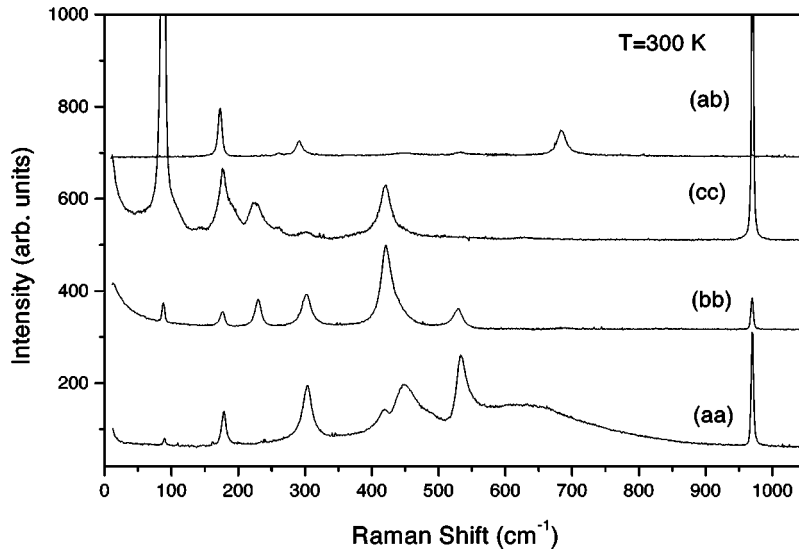
FIG. 1. Room temperature Raman spectra of a α'-NaV$_2$O$_5$ single crystal. Measurements in (cc) polarization were carried out using a micro-Raman setup.

but also intersite Coulomb interaction a charge ordering of the V^{4+}/V^{5+} in a zig-zag structure with diagonal dimers is obtained. This also results in an alternation of the spin exchange constant along the b direction and thus to a spin gap. The charge ordering is thereby driven by the interaction with the lattice distortions and intersite Coulomb interaction. A similar ansatz used by Seo and Fukuyama[22] neglecting lattice distortions also leads to a dimer formation along the diagonal of the ladder as the energetically preferred ground state of α'-NaV$_2$O$_5$. From the experimental point of view diagonal charge ordering is compatible with a splitting of a triplet branch observed in neutron scattering[23,24] and Raman scattering results presented here.

II. EXPERIMENTAL

Raman experiments were performed using an Ar$^+$-ion laser ($\lambda = 514$ nm) and a HeNe laser ($\lambda = 632.8$ nm) as excitation source and a Dilor XY spectrometer. A nitrogen cooled CCD detector was used for detection of the scattered light. The single crystals were grown using a self-flux method. Two different single crystals were available: One that showed a clear drop at $T_{SP} = 34$ K in susceptibility measurements and another one with a slightly broadened transition due to a small Na deficiency. These samples will be called here sample 1 and sample 2, respectively. The crystals are thin platelets of several mm diameter in the (ab) plane. Therefore all scattering geometries with polarizations within the (ab) plane were easy accessible by light scattering experiments. Other geometries could be probed using micro-Raman at room temperature. The samples were cooled in exchange gas of a standard He-bath cryostat. With this setup light scattering in a temperature range 5 K$\leq T \leq 300$ K was investigated.

III. RESULTS AND DISCUSSION

For the understanding of the observed phase transition and further possible instabilities in α'-NaV$_2$O$_5$ it is important to clarify the high temperature phase. As mentioned above x-ray determination of the crystal structure gives doubtless evidence for only one type of V site at room tem-

perature. This is also confirmed in polarized Raman scattering from phonons. Factor group analysis as described, e.g., in Ref. 25 gives the number of symmetry allowed normal modes in Raman and infrared measurements. There are two formula units of α'-NaV$_2$O$_5$ per unit cell. Therefore one expects 45 modes in Raman scattering. For the noncentrosymmetric space group (C_{2v}^7) one obtains $\Gamma = 15$ A_1 $+ 8$ $A_2 + 7$ $B_1 + 15$ B_2. The A_1 modes should be observable in all ''parallel light polarizations'' in Raman spectroscopy as well as for $\mathbf{E} \| a$ in infrared measurements. Indeed, as for this space group there is no center of inversion symmetry, there is no distinction between even and odd modes. The B_1 modes are observable in (ab) polarization as well as for $\mathbf{E} \| b$. The A_2 and the B_2 modes with selection rules (bc), and (ac), $\mathbf{E} \| c$, respectively, are not observable in our experiment because these polarizations are not accessible with our crystals.

For the centrosymmetric space group (D_{2h}^{13}) there is a center of inversion symmetry leading to a clear distinction between Raman and infrared active modes. One obtains 24 Raman active phonon modes: $\Gamma = 8$ $A_g + 3$ $B_{1g} + 8$ B_{2g} $+ 5$ B_{3g}. The residual 18 modes are infrared active. The A_g modes are observable in parallel light polarizations, i.e., (aa), (bb), and (cc). The B_g modes, on the other hand, appear in ''crossed polarizations.'' In our experiment the (ab) scattering configuration with $3B_{1g}$ modes expected is accessible. Figure 1 shows typical room temperature spectra for the geometries. Table I summarizes the modes and compares them to the predictions for the different space groups. It can be stated that the centrosymmetric space group is consistent with the Raman results. Nevertheless, it cannot be excluded that due to matrix elements effects, i.e., weak polarizability of certain modes, we were not able to detect all of them. However, infrared measurements as shown in Ref. 26 are also in agreement with the above interpretation of the data, especially as there is no intermixing between Raman and infrared modes. This symmetry analysis is valid for temperatures above $T_{CO} = 80$ K. Changes observed at lower temperatures will be discussed below. Our results are in contrast to an investigation of Golubschik et $al.$ favoring the noncentrosymmetric space group (C_{2v}^7).[27]

TABLE I. Phonon frequencies of α'-NaV$_2$O$_5$ at room temperature ($T = 300$ K) in the scattering geometries accessible. For comparison the expected number of modes from the factor group analysis for the space groups C_{2v}^7 and D_{2h}^{13} are given.

Polarization	Phonon frequencies (cm^{-1})								(C_{2v}^7)	(D_{2h}^{13})
(aa)	90	178		304	422	450	530	970		
(bb)	90	178	230	304	422	450	530		15	8
(cc)	90	178			422			970		
(ab)		173		292				692	7	3

Considering the room temperature spectra one finds some unusual features. The first striking point is the occurrence of quasielastic scattered light in (bb) polarization, i.e., with the polarization of the incoming and scattered light along the effective chain direction. This scattering is not observed in (aa) spectra. It vanishes upon cooling the sample below $T = 100$ K. It cannot be explained by the Bose-factor. Indeed, in CuGeO$_3$ a similar quasielastic scattering contribution was found with polarization parallel to the dominant exchange path (chain direction)[28,29] and has been assigned to fluctuations of the energy density of the spin system, a feature which is very general for one-dimensional (1D) quantum spin systems. Furthermore, the phonons both in (aa) and (bb) geometry are broadened and show an asymmetric line shape in the frequency range from ~ 250 to 700 cm^{-1}. This frequency regime corresponds roughly to energies of one to two times J (≈ 320–400 cm^{-1}) pointing to a nonnegligible spin-phonon interaction in this system.

A. Continuum scattering above T_{SP}

The most remarkable signal in the room temperature spectra is nevertheless the broad Gaussian-like band of scattering ranging from 250 to 900 cm^{-1} and centered at about 650 cm^{-1}. Figure 2(a) shows typical spectra in (aa) scattering geometry for several temperatures. Upon cooling to lower temperatures two effects are observed. First, the center of this band shifts toward lower frequencies. The shift is displayed in Fig. 2(b). Second, the intensity of the band decreases in favor of the phonon intensity at 533 cm^{-1}.

This shift of the broad band is nearly linear in temperature down to 100 K. Below 100 K the intensity is too small to be analyzed as the Gaussian-like shape has disappeared. Instead an asymmetric tail of the 533 cm^{-1} phonon toward higher energies remains. This is a remarkable change in the shape of this broad excitation. In addition, its intensity shows a peculiar temperature dependence. A maximum at $T = 150$ K and a consequent drastic drop for lower temperatures is observed as it is shown in Fig. 2(b). The phonon at 533 cm^{-1}, on the other hand, shows a clear increase in intensity with decreasing temperature. To summarize, there is a redistribution of spectral weight for temperatures below 150 K suppressing the continuum scattering in favor of the phonon scattering.

We will discuss several scenarios to explain these experimental findings. First, electric dipole transitions between split crystal field levels, second a two-magnon scattering mechanism, and third possible electron-phonon coupled modes observed in antiferromagnets.

Electric dipole transitions between crystal field split levels of d-electron states as the origin of the broad scattering con-

tribution were suggested by Golubschik *et al.*[27] These transitions between different crystal field levels should be discrete. The broad continuumlike shape observed at high temperatures may due to temperature smearing. Upon decreasing the temperature the discrete nature of the excitations should be recovered. However, this is not observed. In addition, independent of the lineshape, the intensity should not show the observed drastic dependence on temperature.

Two-magnon excitations can also lead to broad scattering bands in Raman scattering. The corresponding Raman process is a frustration-induced four-spinon continuum as observed in CuGeO$_3$.[9,30] However, the polarization selection rules allow its existence only for polarizations of the incident and scattered light parallel to the dominant exchange path.[9] In addition, the observed energy range of the band (250–850 cm^{-1}) is not compatible with the range expected for an exchange coupling constant $J = 480$–560 K in α'-NaV$_2$O$_5$.
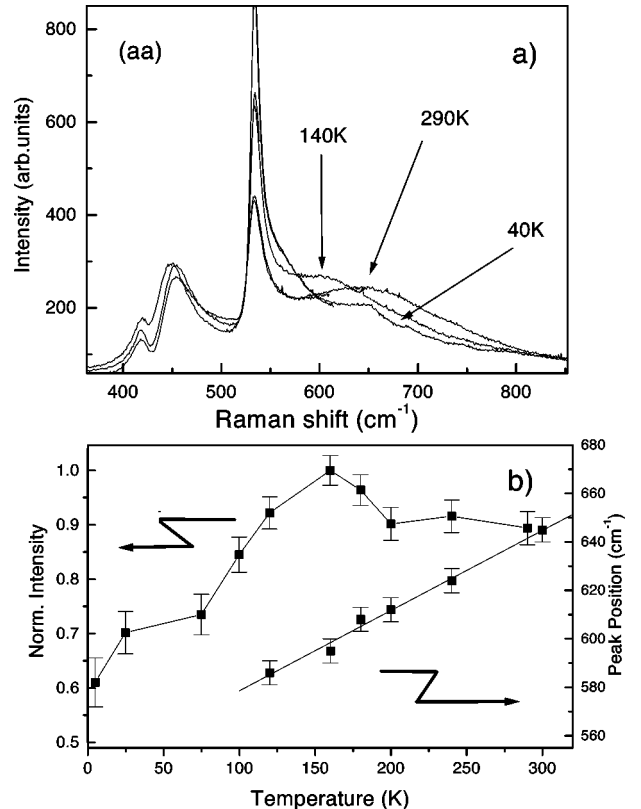
FIG. 2. (a) Broad scattering contribution in (aa) polarization of α'-NaV$_2$O$_5$ at 290, 140, and 40 K. (b) Normalized integrated intensity of the scattering contribution between 565 and 950 cm^{-1} and peak position of the maximum as a function of temperature.

With this J value a maximum centered around 1200–1400 cm^{-1} would be expected.

There are, on the other hand, well comparable experimental results discussed as electron-phonon coupled modes in antiferromagnets (for an overview see Ref. 31). One of the model systems in this respect is FeCl$_2$ with a Néel temperature $T_N = 23.5$ K. In this compound an E_g-phonon at 150 cm^{-1} shows a line shape asymmetry toward higher energy and a broadening for $T \gtrsim T_N$. For $T \lesssim T_N$ the phonon sharpens in linewidth and a broad Gaussian-like excitation band is observed on the high frequency side that shifts towards higher frequencies upon cooling further down well below T_N. This band is due to a resonant electron-phonon interaction between a Fe^{2+} d level and the E_g phonon. The shift of the maximum observed in α'-NaV$_2$O$_5$ is opposite to these observations in FeCl$_2$. This difference in the two classes of materials concerning the electron-phonon coupled modes is connected with the strong spin fluctuations in low dimensions. In the dimerized state of a low dimensional spin system the spin-spin correlation length decays exponentially and is therefore always smaller than in the homogeneous state with algebraically decaying correlations. This decrease of the correlation length is just opposite to the behavior of an antiferromagnet cooled below the Néel temperature. This leads to the reversed temperature dependence of the electron-phonon coupled modes in the two different materials.

More general, in systems with low energy excitations electronic satellites might appear on the high-energy side of a phonon if the low-energy excitations and the phonon couple to the same electronic state. This has been observed in Raman scattering on Tl$_2$Ba$_2$CuO$_6$.[32] As the broad band in α'-NaV$_2$O$_5$ is observed only for (aa) polarization it serves as a strong experimental evidence that there are additional low energy excitations in the a direction, i.e., perpendicular to the ladder legs. Further theoretical investigations of this phenomenon are desirable, especially concerning its peculiar temperature dependence, as it will give valuable insight in the microscopic couplings between electronic and phononic degrees of freedom in the high-temperature phase of this compound.

B. Magnetic bound states

In the low-temperature phase ($T \lesssim T_{SP}$) several new modes do appear in polarizations along the "chains" (bb) (see Fig. 3), and perpendicular to them (aa) as well as in crossed polarization (ab).[33] A survey of the frequencies of the additional modes is shown in Table II. Comparing the temperature dependence of the intensity, frequency and half-width of the additional modes we come to a clear distinction between the three modes at the lowest energies, i.e., at 67, 107, and 134 cm^{-1} and the other transition-induced modes. The 67 and 134 cm^{-1} modes appear in (aa), (bb), and (ab) polarization, while the 107 cm^{-1} mode is observed only in (bb) polarization. Figure 4 shows the temperature dependence of the normalized integrated intensity of the modes at 67, 107, 134, 202, 246, and 948 cm^{-1} as observed in (bb) scattering geometry. The latter three modes follow the behavior expected from ordinary phonons that are folded from the zone boundary to the zone center. Cooling down from high temperatures the intensities rise sharply below T_{SP}
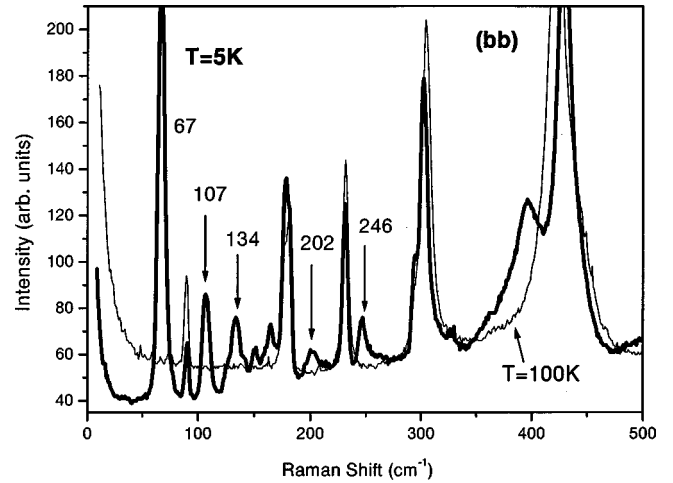
FIG. 3. Low-temperature modes of α'-NaV$_2$O$_5$ in (bb) scattering geometry: transition-induced modes with frequencies below 500 cm^{-1}. The thick (thin) line corresponds to measurements at $T = 5$ K (100 K). Note the drop in background intensity for frequencies smaller than 120 cm^{-1} corresponding to $2\Delta_{ST}$.

and then saturate. The three low frequency modes obviously do not behave like this. They increase more gradually upon cooling with a smaller slope and show no saturation in intensity toward the lowest temperature. Moreover, these three modes get broader and soften toward lower frequencies upon approaching T_{SP} from low temperatures.[33] So these modes really vanish above T_{SP} and are obviously closely connected to the opening of an energy gap in the magnetic excitation spectrum. This is in contrast to the modes at 202, 246, and 948 cm^{-1} which do neither show any broadening nor any shift in frequency upon approaching T_{SP} from below. They can therefore be assigned to phonons which exist also above T_{SP}, but become Raman active due to the lowering of the symmetry for $T \lesssim T_{SP}$.

This conclusion is in close analogy to the situation in the spin-Peierls compound CuGeO$_3$ where a similar distinction between a mode at 30 cm^{-1} and dimerization-induced folded phonon modes could be made. The 30-cm^{-1} mode was assigned to a bound singlet state of two triplet excitations. The frustration induced binding of the triplets leads to its energy below the two-triplet continuum of states.[10,34] The linear intensity increase with decreasing temperatures below T_{SP} results from the gradually developing order parameter as a prerequisite of a composite state of two triplets. In this way CuGeO$_3$ serves as a model system concerning the occurrence of such magnetic bound states.

Nevertheless, the existence of such states is a quite general feature of low-dimensional spin systems with a gapped excitation spectrum. We therefore assign the three modes at 67, 107, and 134 cm^{-1} to magnetic singlet bound states. With $\Delta_{ST} = 85$ K $\equiv 60$ cm^{-1} from susceptibility measurements these three modes are situated below or near $2 \times \Delta_{ST}$. This gap value is also confirmed in our Raman measurements as a drop in the background intensity below 120 cm^{-1}. The number and selection rules of the singlet bound states, however, differ from what has been observed in CuGeO$_3$ pointing to a different ground state and excitation scheme in α'-NaV$_2$O$_5$. We will discuss this point below.

TABLE II. Additional low temperature modes of α'-NaV$_2$O$_5$ for $T \leqslant T_{SP}$ in various scattering geometries. For comparison the frequencies of the modes in sample 2 are given in brackets.

Polarization	Low-temperature modes (cm^{-1}) for $T \leqslant T_{SP}$					
(aa)	67(64)		133(130)			
(bb)	67(64)	107(103)	134(131)	151	164(164)	202(202)
(ab)	67(64)		134(131)			
(aa)				650(650)	692(692)	948(947)
(bb)	246(244)	325(325)	394(394)			948(948)
(ab)						948(948)

Now one may raise objections against the interpretation of the modes as magnetic bound states. The first objection might be that the 67-cm^{-1} mode is comparable in frequency to the singlet-triplet energy gap ($\Delta_{ST} = 60$ cm^{-1}) and might therefore be just the one-magnon scattering which might be allowed due to spin-orbit coupling. However, the g-value in α'-NaV$_2$O$_5$ is even closer to 2 than in CuGeO$_3$,[12,35] pointing to a negligible orbital momentum in this compound. Furthermore, if the 67-cm^{-1} mode would be interpreted as a one-magnon scattering, the 134-cm^{-1} mode may then be understood as the corresponding two-magnon scattering.[36] This, however, would be surprising since two-magnon scattering is strongly renormalized to lower frequencies already in two dimensional spin systems.[37]

A very important test on relevant spin-orbit coupling is the application of a magnetic field. This should lift the three-fold degeneracy of the triplet state, resulting in a splitting and a shift of this mode. Figure 5 shows the 67-cm^{-1} mode measured in a magnetic field of 0, 4, and 7 T$\equiv$6.6 cm^{-1}. We neither observe a shift nor a splitting nor even a broadening of the 67-cm^{-1} mode. Therefore such a simple one-magnon interpretation can be clearly ruled out.

On the other hand, one might also suggest that our three bound states are not of magnetic but rather of phononic origin. Indeed, such phonon bound state phenomena have been observed for example in YbS.[38,39] There, these modes were interpreted as excitons interacting with an LO phonon of frequency ω_0 giving rise to exciton-phonon bound states with frequencies $\omega = n \times \omega_0$, with n an integer and polarization selection rules identical with the original LO phonon. Finally, the linewidth of these bound states is a linear function of n. The first property can be found in our system on assuming an ω_0 of about 30 cm^{-1}. However, no such phonon mode could be detected. Besides, the scattering intensity of the bound states in α'-NaV$_2$O$_5$ appears not only in the fully symmetric scattering components (aa), (bb), but also in (ab). A similar disagreement is found for the linewidth that does not show a systematic broadening with n. Clearly, these experimental results are not compatible with our observations in α'-NaV$_2$O$_5$.

We will now use results on the Na deficient sample 2 to confirm the above made analysis and to prove that the energy of the bound states is closely related to the singlet-triplet gap.

FIG. 4. Temperature dependence of the normalized integrated intensity of the transition-induced modes in α'-NaV$_2$O$_5$. The three modes at 67, 107, and 134 cm^{-1} (closed symbol) show a temperature dependency different from the modes observed at higher frequencies.
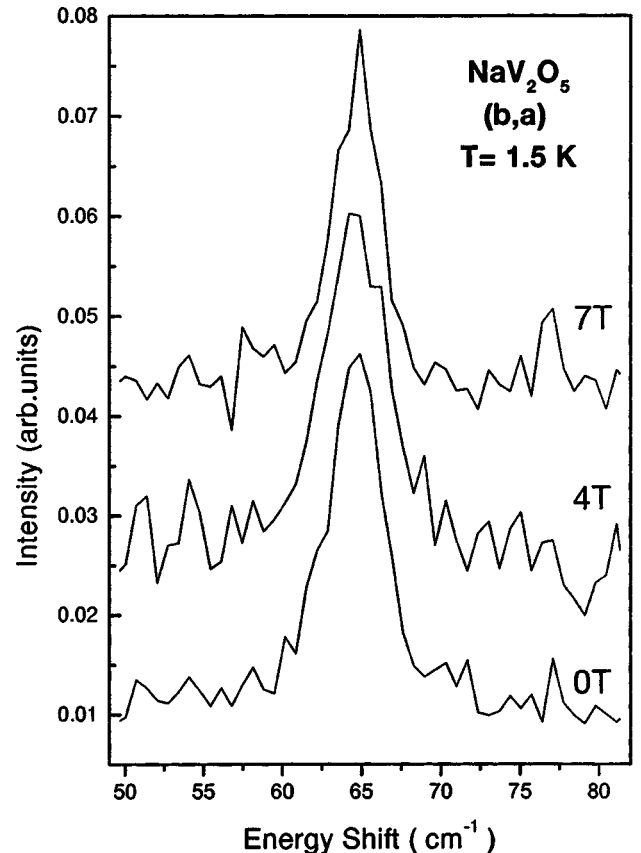
FIG. 5. Behavior of the 67-cm^{-1} mode upon applying a magnetic field of 0, 4, and 7 T. This measurement was performed using a Brillouin Fabry-Perot spectrometer.

FIG. 7. Comparison of the (aa) spectra of α'-NaV$_2$O$_5$ at 5 K for $\lambda = 514.5$ nm and $\lambda = 632.8$ nm.
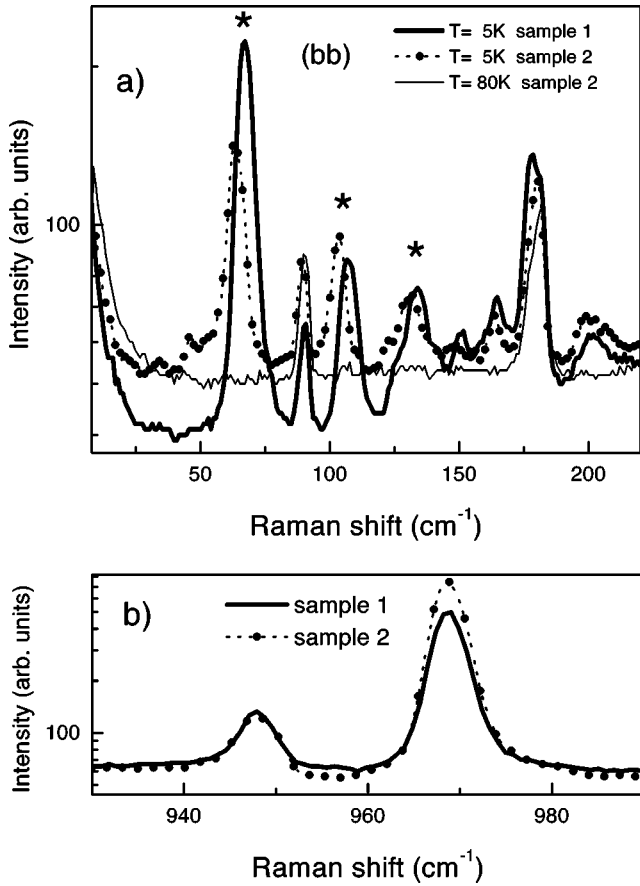
FIG. 6. Comparison between sample 1 and the 1 % Na deficient sample 2 of α'-NaV$_2$O$_5$ at $T = 5$ K. Additionally a measurement of sample 2 at $T = 80$ K is given in (a). The scattering intensity is displayed on a logarithmic scale. The magnetic bound states in (a) marked with an asterisk show a considerable shift toward lower frequencies with Na deficiency while the modes at 202 cm^{-1} in (a) and 948 cm^{-1} in (b) stay constant in frequency. Please note that the decrease of the background scattering intensity of sample 1 for frequencies below $2\Delta_{ST} = 120$ cm^{-1} is suppressed by the Na deficiency of sample 2.

One of the most subtle problems preparing α'-NaV$_2$O$_5$ samples is to control the Na content. Deviations from the nominal stoichiometry result in a shift of the ratio between V^{4+} and V^{5+} toward the nonmagnetic ($S = 0$) V^{5+}. This then acts as an effective substitution. Systematic studies of Na deficiencies as reported in Ref. 40 indeed show that the drop in the magnetic susceptibility is suppressed and T_{SP} is slightly shifted toward lower temperatures. Comparing the data in Ref. 40 with the susceptibility data of our sample 2 we come to the conclusion that the latter has about 1% Na deficiency. In principle, both samples show the same Raman scattering results both in the high temperature and the dimerized phase. In the dimerized phase the frequencies of most transition-induced modes are the same for both samples within the experimental resolution. Solely, the three low-frequency modes show a considerable shift in frequency to 64 (67), 103 (107), and 130 (134) cm^{-1}, with the values of sample 1 given in brackets. A direct comparison of the $T = 5$ K spectra of sample 1 and 2 in (bb) polarization is shown in Fig. 6. Clearly, the modes at 202, 246 (not shown), and 948 cm^{-1} attributed to zone folded phonon modes do
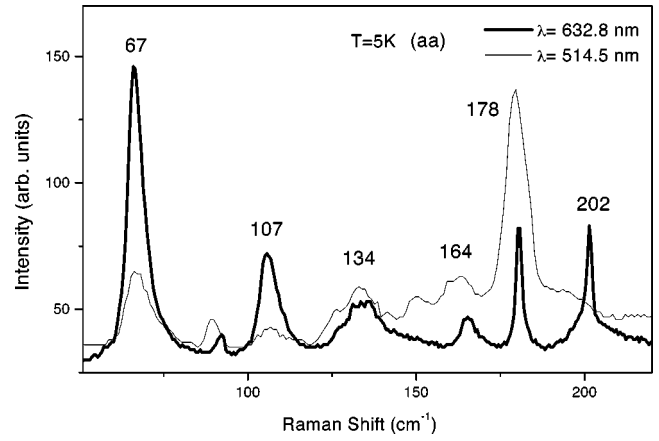
not show this shift towards lower frequencies. The frequency shift of the bound states is explained quite naturally by assuming that the Na deficiency of sample 2 leads to a reduced singlet-triplet gap and hence to a smaller energy of the magnetic bound states. Actually, a similar behavior has been observed in Zn-substituted CuGeO$_3$.[10]

Further insight into the underlying physics of the low-temperature excitations can be gained from resonance Raman measurements. By changing the frequency of the incident laser light from $\lambda = 514.5$ nm (2.5 eV) to $\lambda = 632.8$ nm (1.9 eV) one observes a different response of the phonon intensity and the three magnetic bound states. Figure 7 shows the low frequency part of the (aa) spectrum at 5 K for $\lambda = 514.5$ and $\lambda = 632.8$ nm. It can be clearly stated that compared to both the high temperature mode at 178 cm^{-1} and the folded phonon mode at 164 cm^{-1} the three magnetic bound states at 67, 107, and 134 cm^{-1} gain intensity for excitation at smaller wavelength. This again underlines our above made distinction between modes of phononic and modes of magnetic origin as the magnetic excitations are coupled differently to the optical excitation.

The dependence of the gained scattering intensity on the frequency of the incident laser light can easily be understood in the way that there are different electronic transitions involved as intermediate states in the Raman process. Roughly speaking, the scattering intensity I in a two-band approximation should behave as $I \sim 1/(\omega - \Delta_{ET})^p$, with ω the frequency of the incident laser light and Δ_{ET} the energy of the electronic transition involved. The parameter p depends on the order of the scattering process.

C. Ground state properties of α'-NaV$_2$O$_5$

It can be stated that the modes at 67, 107, and 134 cm^{-1} can be described best as magnetic singlet bound states. They, however, do not fit both in number and in selection rules to the excitation spectrum of a frustrated and dimerized 1D Heisenberg chain, which exhibits only one singlet bound state. The intensity of this singlet bound state should only be observed with polarizations parallel to the dominant exchange path, i.e., along the chain direction.

In the high-temperature phase ($T \geq T_{SP}$) α'-NaV$_2$O$_5$ is described as a quarter-filled Hubbard ladder. As the charge

transfer gap $\Delta_{CT} \approx 1$ eV is large the low energy excitations are dominated by spin fluctuations of one spin per rung along the ladder direction. This leads to a mapping of the system on a spin 1/2 Heisenberg chain.[17] Actually, the mode at 107 cm^{-1} does match both in selection rules (only observable with polarization of the incoming and scattered light along the ladder direction) and in energy (107 cm$^{-1} = 1.78 \times \Delta_{ST}$) the singlet bound state in CuGeO$_3$ (30 cm^{-1} $= 1.76 \times \Delta_{ST}$). Therefore we can understand this mode as the singlet bound state of the effective dimerized chain. However, there are two further bound states at 67 and 134 cm^{-1} which are unpolarized in the *ab* plane.

This breaking of the selection rules expected for an effective chain system may be understood if the full geometry of the Heisenberg ladder is taken into account. This means that both dimers along the ladder diagonal as well as dimers along and perpendicular to the ladder exist. As the observed bound states have a small energy separation compared to $\Delta_{CT} \approx 1$ eV the underlying dimers should be energetically nearly degenerate. Actually, their energy scale is given by the singlet-triplet gap $\Delta_{ST} \approx 9.8$ meV.[23] Therefore the character of the excitations is predominantly magnetic allowing a description of the bound states in the context of a pure spin model.

Furthermore, as the bound states are unpolarized no preferred dimer configuration exists. The small energy separation therefore allows for a dynamic dimer formation as the new ground state of this system. In this way one can both explain the unexpected multiplicity and the breakdown of the selection rules.[33] There exists a close analogy of this picture to the dynamical Jahn-Teller or the RVB model. The superposition of different energetically nearly degenerate dimer configurations should also show up in the triplet channel of the excitation spectrum. In fact, recent neutron scattering studies[23] revealed an unexpected splitting of the dispersion of the triplet excitations along the *a* axis. This is consistent with our considerations as there are dimers not only in chain direction but also perpendicular to it. Further theoretical support of our point of view comes from two recent works[22,21] assuming a zig-zac chain structure corresponding to diagonal dimers as the ground state for $T < T_{SP}$. Due to charge ordering driven by intersite-Coulomb interaction such a zig-zag type of charge disproportionation along the ladders occurs leading to dimers which are not only situated along the chain direction.

D. Charge ordering

Despite the above explanation of the low energy Raman spectrum in terms of a spin model with resonating dimer configurations the underlying mechanism that drives the system into the dimerized ground state is nevertheless still under discussion. One of the key questions is whether a charge ordering occurs and whether its energy scale is constrained by the large Δ_{CT}. Furthermore, it should be clarified whether charge ordering appears instantaneously with the singlet formation or whether two distinct consecutive transitions can be observed.

Experimental evidence for a charge ordering is given by the observation of two distinctly different V sites below T_{SP} in NMR spectroscopy.[41] In thermal expansion data a double
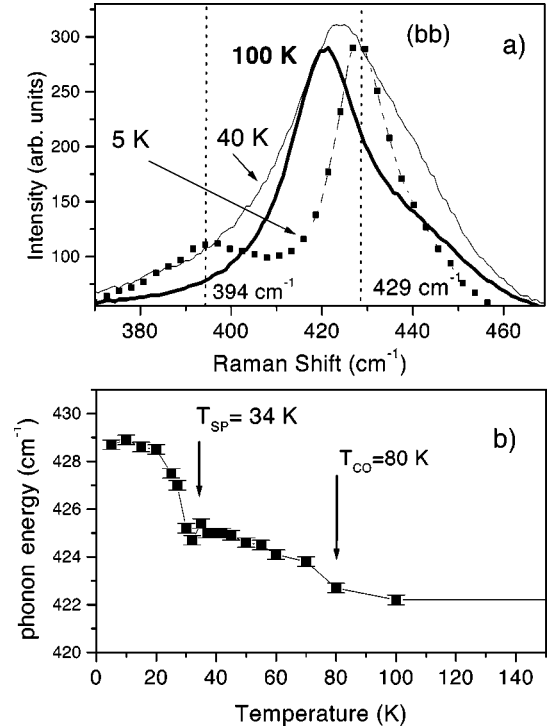
FIG. 8. Temperature dependence of the energy of the 422-cm^{-1} mode of α'-NaV$_2$O$_5$ in (*bb*) polarization: (a) Scattering intensity and (b) phonon energy. For temperatures below 22K a second peak develops near 394 cm^{-1}. The temperature dependence of the mode at 422 cm^{-1} marks the onset of charge ordering at $T_{CO} = 80$ K.

phase transition has been observed in a very small temperature interval near $T = 34$ K.[42] However, the interpretation of the data is not unambiguous. On the other hand, recent infrared measurements point towards a temperature scale different from T_{SP} because of the finite intensity of a spin-Peierls active phonon for temperatures as high as 60–70 K.[26] Recent ultrasonic experiments[43] report a transition induced anomaly in the longitudinal sound velocity along the chain direction extending up to $2 \times T_{SP} \approx 70$ K. On the low-temperature side the transition appears to be much sharper. Indeed, the velocity anomaly disappears again only at $0.8 \times T_{SP} = 27$ K. This corresponds to the temperature at which the magnetic modes start to develop in the Raman spectra supporting their interpretation as magnetic bound states that need to have a well developed order parameter.

At room temperature all the V sites have formally the valence +4.5. In this case a *z*-axis vibration (out of the *ab* plane) of the V ions within one rung should be Raman silent if the ions move out-of-phase. At the same time, the corresponding in-phase vibration is Raman active. A charge disproportionation within a rung can manifest itself in Raman scattering as the appearance of a new intense mode. This mode is related to V ion vibrations accompanied by a considerable shift in frequency of other V-related modes. This shift occurs mainly due to ordering-induced changes in the Coulomb contribution to the lattice force constants. Experimentally, we observe such a behavior of a phonon in A_g symmetry at 422 cm^{-1} that shifts to 429 cm^{-1} at lower temperatures with an additional split-off mode at 394 cm^{-1}. Figure 8 shows these modes in (*bb*) scattering geometry, which we suppose to be the in-phase *z*-axis vibration of the
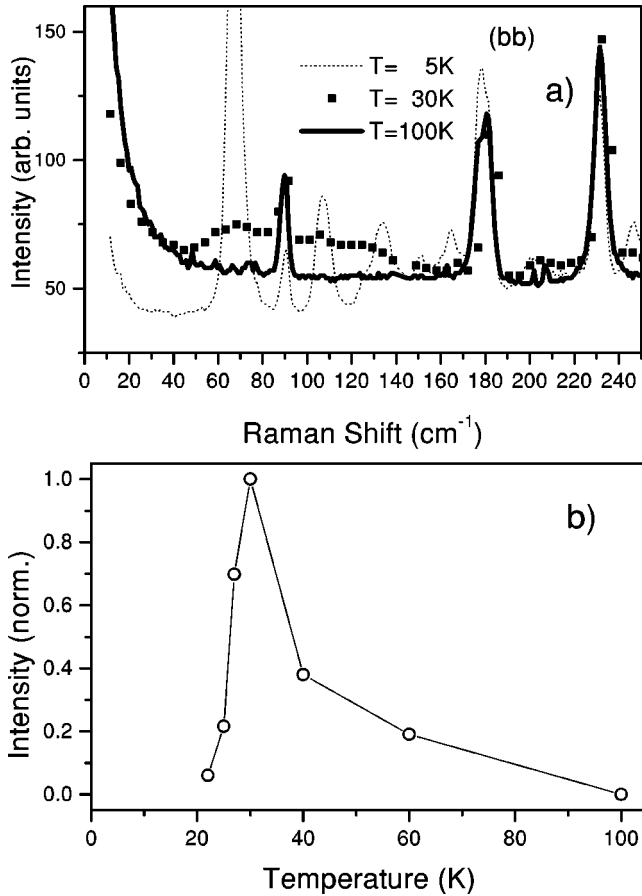
FIG. 9. (a) Additional scattering contribution of α'-NaV$_2$O$_5$ at 30 K in the low frequency range (40–160 cm^{-1}) in (bb) polarization and (b) temperature dependence of its integrated intensity.

V ions within a rung. In the case of charge asymmetry, the normal coordinates are linear combinations of the in-phase and out-of-phase vibrations and, therefore a new ''in-phase'' mode appears in the Raman spectrum. If the mixing is strong enough, each one of the new modes can be interpreted as a vibration of one V ion. Below T_{SP} the frequency of the intense peak shifts to 429 cm^{-1} at 5 K. Comparing the temperature dependencies of the frequency and the intensity of this additional phonon below T_{SP} it can be stated that the onset of the hardening is well above this temperature.

The amount of hardening can roughly be estimated quantitatively. We define the Coulomb contribution to the force constant $k_{Coulomb}$ as the second derivative of the Coulomb energy with respect to the z-displacement of the V ion for its interaction with the apical oxygen above the V ion and the nearest-neighbors in the (ab) plane. Thereby we get $k_{Coulomb} \approx 2.5 \times 10^5$ erg/cm^2.[44] The measured effective k for this mode can be estimated by $k_{exp} = M\Omega^2$ with M the V ion mass and $\Omega = 420$ cm^{-1}, to $k_{exp} \approx 6 \times 10^5$ erg/cm^2. The difference k_{exp}-$k_{Coulomb}$ should be attributed to a further contribution due to the covalent bonding $k_{bonding}$: $k_{exp} = k_{Coulomb} + k_{bonding}$. This contribution of $k_{bonding}$ between a V ion and the apical O should not be too much affected by a charge ordering. The charge asymmetry, on the other hand, changes the charge of one of the V ions from +4.5 to +5, i.e., $\tilde{k}_{Coulomb} = k_{Coulomb} \times 1.1$. With this value one can estimate the new frequency $\tilde{\Omega} = \sqrt{\tilde{k}/M}$. The corresponding shift $\tilde{\Omega} - \Omega$ that should be

observable as function of temperature is then 2% or ≈ 8 cm^{-1}. This corresponds roughly to the shift of the mode from 422 to 429 cm^{-1}.

A new peak appears in the dimerized phase at 394 cm^{-1} as a shoulder of the 429 cm^{-1} mode. We attribute this peak to the vibration originating from the silent mode. It then can be assigned to arising from the scattering mainly by V^{4+} vibrations, whereas the peak at 429 cm^{-1} is due to the V^{5+} vibrations. The splitting of the frequencies is due to a direct interaction of the V ions. The diminished intensity of the peak at 394 cm^{-1} compared to the 429-cm^{-1} mode can qualitatively be understood by taking into account that V^{4+} possesses one more electron compared to V^{5+}. Therefore, a virtual transition of an electron to this ion requires an additional energy due to the Coulomb repulsion with the d electron already there. If the photon energy is out of resonance with this transition, this Hubbard-like term will diminish the scattering intensity of the V^{4+} vibration at 394 cm^{-1}.

It is worth mentioning that the charge ordering can hardly be considered as static since the phonons can drive strong fluctuations of the V ion charge. Let us consider the situation in more details at the beginning for $T > T_{SP}$. The d electrons are in the strong Coulomb field of the apical oxygen above the V ion. In the out-of-phase vibration the V ions become nonequivalent, and the field causes strong charge transfer between them. The relative value of the charge transfer $\Delta Q/\bar{Q}$ can be estimated as $eE_a z_0/t_\perp$, where e is the electron charge, E_a is the electric field between the apical oxygen and the V ion, z_0 is the zero-point vibrational amplitude, $t_\perp$ is the a-direction hopping perpendicular to the ladder, and $\bar{Q}$ = 1/2. Taking as estimate $E_a \approx 2e/d_0^2 \approx 4 \times 10^6$ cgs units, with $d_0 \approx 1.6$ Å the distance between the V and apical oxygen ions, the zero-point vibrational amplitude $z_0 = \sqrt{\hbar/2M\Omega} \approx 0.03$ Å, with $\Omega \approx 422$ cm^{-1} and $t_\perp \approx 0.35$ eV,[18] we obtain $\Delta Q/\bar{Q} \sim 1$. This implies very strong phonon-driven charge fluctuations.[44] Since the superexchange is determined by the hopping of electrons between the rungs, these charge fluctuations, in turn, cause fluctuations of the exchange parameter J, leading to a considerable spin-phonon coupling.[45,46] In the low-temperature phase the charge fluctuations are smaller than above T_{SP}. However, they are still strong enough to make the ordering non-static. Therefore the fluctuations have to be considered as one of the driving forces for dynamical dimer configurations as manifested in the multiplicity of the observed magnetic bound states.

The temperature dependent frequency shift of the 422 cm^{-1} mode displayed in Fig. 8 shows that this charge ordering partly exists above T_{SP}. At these temperatures the ordering can occur as zigzag-like fluctuations of V ions charges in parts of the ladders. Therefore a crossover temperature of $T_{CO} = 80$ K is defined as the onset of the frequency shift compared to higher temperatures. This smooth crossover is typical for charge ordering in 1D. A similar behavior has been observed in neutron diffraction studies of stripe ordering in La$_2$NiO$_{4+\delta}$.[47] The super structure peaks corresponding to stripes of charges and of spins appear in this compound separated in temperature for $T \lesssim T_{CO} = 200$ K and $T \lesssim T_m = 110$ K, respectively. The appearance of T_{CO} in the temperature dependence of the superlattice
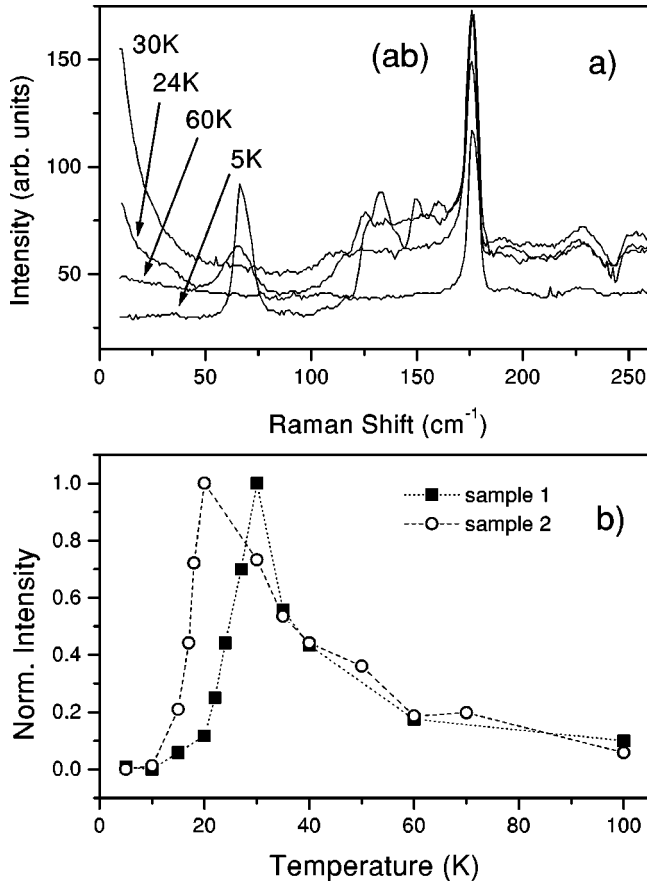
FIG. 10. Quasielastically scattered light of α'-NaV$_2$O$_5$ below T_{CO} observed in (ab) polarization. (a) Spectra of sample 1 for different temperatures. (b) Temperature dependence of the normalized integrated intensity comparing sample 1 and sample 2.

intensity is identical to our observations in α'-NaV$_2$O$_5$. As $T_{CO}=200$ K exceeds T_m by a factor of 2 charge ordering is proposed to be the driving force of this phenomenon in La$_2$NiO$_{4+\delta}$.[48] The same conclusion should hold for α'-NaV$_2$O$_5$ as here charge ordering appearing below $T_{CO}=80$ K sets the scale for the following singlet formation at $T=34$ K.

E. Fluctuations above the singlet ground state formation

Now the question arises whether the charge ordering might also show up in fluctuations in the magnetic light scattering. We will present two further low frequency scattering contributions that are detected for temperatures below T_{CO} and assigned in that way. In Fig. 9 the low frequency part of the (bb) spectrum is presented for $T=5$, 30, and 100 K. At 100 K only the high-temperature phonons at 90, 178, and 223 cm^{-1} are observed. For $T=5$ K this spectrum is modified due to the existence of the additional low-temperature modes. On the contrary, for $T=30$ K one finds a broad scattering contribution from 40 to 160 cm^{-1}. This scattering contribution arises for temperatures below 80 K and peaks in intensity at about 30 K [Fig. 8(b)]. With the low frequency modes emerging below T_{SP} the intensity of this broad contribution drops again. There is this clear competition between the broad low frequency scattering contribution and the magnetic bound states both in their intensity as function of tem-
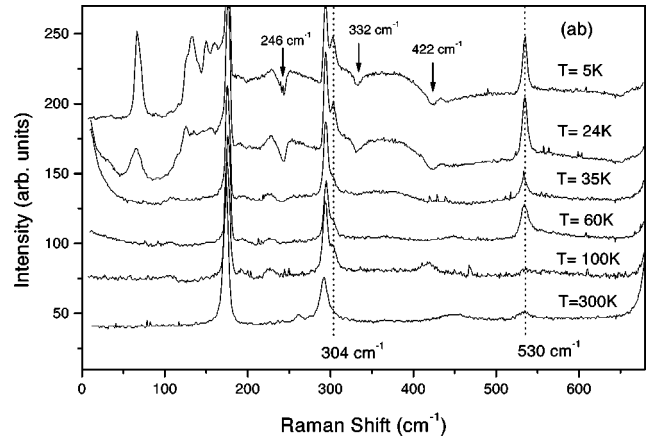
FIG. 11. Raman spectra of α'-NaV$_2$O$_5$ in (ab) polarization for several temperatures. For clarity the spectra are shifted against each other. For $T<60$ K symmetry forbidden A_{1g} phonons evolve at 304 and 530 cm^{-1}. Below T_{SP} there are three dips (antiresonances) in the scattering continuum at 246, 332, and 422 cm^{-1} which coincide in frequencies with phonon modes observed in (bb) polarization; the first two modes are folded zone boundary phonons for $T<T_{SP}$.

perature and in the common frequency range. Therefore, it appears straightforward to assign this contribution to magnetic light scattering that is suppressed for $T \lesssim T_{SP}$.

A second observation of pretransitional fluctuations exists in the low frequency data in (ab) scattering geometry. The Raman data in this geometry is presented as a function of temperature in Fig. 10(a). A quasielastic scattering contribution is observed which again increases below 80 K peaking near T_{SP}. Again this contribution is suppressed at lower temperatures due to the appearance of the magnetic bound states. In Fig. 10(b) the temperature dependence of this intensity is shown. Clearly, it exhibits the same behavior as the broad contribution in (bb) polarization [Fig. 8(b)]. For comparison we have included the temperature dependence of the sample 2 which has a 1% Na deficiency. Here the transition region appears to be broadened and the maximum signal occurs at lower temperatures compared to sample 1. However, it is important to note that the drop in this quasielastic light scattering contribution light does not coincide with T_{SP} but rather with the occurrence of the magnetic bound states. These states emerge at considerable lower temperatures compared to the zone-folded phonons. Therefore this quasielastic scattering contribution can be clearly identified as originating from magnetic Raman scattering. In this sense the $\omega \sim 0$ scattering as well as the broad contribution in (bb) scattering geometry can be understood as dimer fluctuations in a charge ordered state. The main difference between both effects is that the $\omega \sim 0$ scattering in (ab) polarization is gapless.

A further phonon anomaly on the temperature scale of $T_{CO}=80$ K is displayed in Fig. 11. For the centrosymmetric space group D_{2h}^{13} the (ab) spectrum should show only B_{1g} modes. For the room temperature spectrum this is actually the case. There are essentially only three modes at 173, 292, and 692 cm^{-1} (not shown) in agreement with the factor group analysis. However, already for temperatures below ~ 100 K a significant contribution of the A_{1g} mode at 530 cm^{-1} can be detected. Also the 304 cm^{-1} mode gradu-

ally appears. Such an appearance of symmetry forbidden A_{1g} modes can be understood presuming a breakdown of the inversion symmetry due to charge ordering at this temperature. Actually, in the (ab) spectrum at 5 K one can see not only the above mentioned A_{1g} modes but furthermore also some dips in the broad continuum at 246, 332, and 422 cm^{-1}. These antiresonances origininate from phonons observed in the (bb) spectrum. This points to an interaction between these phonons and the two-triplet continuum in (ab) polarization. Finally, the B_{1g} mode at 692 cm^{-1} is also visible in the (aa) spectrum in the dimerized phase. Thus the charge ordering does not only show up in the magnetic scattering but also in the lattice degrees of freedom.

IV. CONCLUSIONS

We have performed Raman scattering studies on α'-NaV$_2$O$_5$. Room temperature phonon scattering is in agreement with a crystal structure that leads to a quarter-filled ladder as the appropriate underlying physical model. The transition-induced modes ($T \leqslant T_{SP}$) are divided into magnetic bound states at 67, 107, 134 cm^{-1} and zone boundary folded phonons. The properties of the bound states lead us to the conclusion that the ground state of this system can be understood as a superposition of various nearly degenerate dimer configurations. As the energy scale of the bound states is comparable to the singlet triplet gap their predominantly magnetic character is concluded, allowing a discussion within purely magnetic spin models. The phase transition into this ground state is initiated by a charge or-

dering of the V^{4+}/V^{5+} ions occurring as a smooth crossover at temperatures higher than T_{SP}. Experimental evidence for such a charge ordering is found as an anomalous hardening and splitting of a V vibration at 422 cm^{-1}. This hardening sets in at a crossover temperature $T_{CO} = 80$ K and is accompanied by fluctuations which were identified in a quasielastic scattering in (ab) scattering geometry and a broad continuum extending from 40 to 160 cm^{-1} in the (bb) scattering contribution. The onset of a charge ordering is further supported by a breakdown of phonon selection rules for $T \leqslant 100$ K. The subtle interplay of charge and spin degrees of freedom manifests itself in α'-NaV$_2$O$_5$ in a transition into a dimerized ground state at $T_{SP} = 34$ K which is initiated by a charge ordering for temperatures below $T_{CO} = 80$ K, as well as in a rich excitation spectrum. Therefore the concluded similarities with the behavior of La$_2$NiO$_{4+\delta}$ or quasi-one-dimensional conductors are far from being accidental. These partially filled low-dimensional systems are all governed by Coulomb correlations.

[1] E. Pytte, Phys. Rev. B **10**, 4637 (1974).

[2] M. C. Cross and D. S. Fisher, Phys. Rev. B **19**, 402 (1979).

[3] For a review, see J. W. Bray, L. V. Interrante, I. S. Jacobs, and J. C. Bonner, in *Extended Linear Chain Compounds*, edited by J. S. Miller (Plenum, New York, 1983), Vol. 3, pp. 353-415.

[4] M. Hase, I. Terasaki, and K. Uchinokura, Phys. Rev. Lett. **70**, 3651 (1993).

[5] M. Nishi, O. Fujita, and J. Akimitsu, Phys. Rev. B **50**, 6508 (1994).

[6] G. Castilla, S. Chakravarty, and V. J. Emery, Phys. Rev. Lett. **75**, 1823 (1995).

[7] For a review, see J. P. Boucher and L. P. Regnault, J. Phys. I **6**, 1 (1996).

[8] H. Kuroe, T. Sekine, M. Hase, Y. Sasago, K. Uchinokura, H. Kojima, I. Tanaka, and Y. Shibuya, Phys. Rev. B **50**, 16 468 (1994).

[9] V. N. Muthukumar, C. Gros, W. Wenzel, R. Valenti, P. Lemmens, B. Eisener, G. Güntherodt, M. Weiden, C. Geibel, and F. Steglich, Phys. Rev. B **54**, R9635 (1996).

[10] P. Lemmens, M. Fischer, G. Güntherodt, C. Gros, P. G. J. van Dongen, M. Weiden, W. Richter, C. Geibel, and F. Steglich, Phys. Rev. B **55**, 15 076 (1997).

[11] V. N. Kotov, O. P. Sushkov, and R. Eder, Phys. Rev. B **59**, 6266 (1999).

[12] M. Isobe and Y. Ueda, J. Phys. Soc. Jpn. **65**, 1178 (1996).

[13] M. Weiden, R. Hauptmann, C. Geibel, F. Steglich, M. Fischer, P. Lemmens, and G. Güntherodt, Z. Phys. B **103**, 1 (1997).

[14] Y. Fujii, H. Nakao, T. Yosihama, M. Nishi, K. Nakajima, K. Kakurai, M. Isobe, Y. Ueda, and H. Sawa, J. Phys. Soc. Jpn. **66**, 326 (1997).

[15] J. Galy, A. Casalot, M. Pouchard, and P. Hagenmuller, C. R. Seances Acad. Sci., Ser. C **262**, 1055 (1966).

[16] H. G. v. Schnering, Yu. Grin, M. Kaupp, M. Somer, R. K. Kremer, O. Jepsen, T. Chatterji, and M. Weiden, Z. Kristallogr. **213**, 246 (1998).

[17] H. Smolinski, C. Gros, W. Weber, U. Peuchert, G. Roth, M. Weiden, and C. Geibel, Phys. Rev. Lett. **80**, 5164 (1998).

[18] P. Horsch and F. Mack, Eur. Phys. J. B **5**, 367 (1998).

[19] H. Seo and H. Fukuyama, J. Phys. Soc. Jpn. **66**, 1249 (1997).

[20] P. Thalmeier and P. Fulde, Europhys. Lett. **44**, 242 (1998).

[21] M. V. Mostovoy and D. I. Khomskii, cond-mat/9806215 (unpublished).

[22] H. Seo and H. Fukuyama, cond-mat/9805185 (unpublished).

[23] T. Yoshihama, M. Nishi, K. Nakajima, K. Kakurai, Y. Fujii, M. Isobe, C. Kagami, and Y. Ueda, J. Phys. Soc. Jpn. **67**, 744 (1998).

[24] C. Gros and R. Valentí, Phys. Rev. Lett. **82**, 976 (1999).

[25] D. L. Rousseau, R. P. Bauman, and S. P. S. Porto, J. Raman Spectrosc. **10**, 253 (1981).

[26] A. Damascelli, D. van der Marel, M. Grüninger, C. Presura, T. T. M. Palstra, J. Jegoudez, and A. Revcolevschi, Phys. Rev. Lett. **81**, 918 (1998).

[27] S. A. Golubschik, M. Isobe, A. N. Ivlev, B. N. Mavrin, M. N. Popova, A. B. Sushkov, Y. Ueda, and A. N. Vasilev, J. Phys. Soc. Jpn. **66**, 4042 (1997).

[28] I. Yamada and H. Onda, Phys. Rev. B **49**, 1048 (1994).

[29] H. Kuroe, J. Sasaki, T. Sekine, N. Koide, Y. Sasago, K. Uchinokura, and M. Hase, Phys. Rev. B **55**, 409 (1997).

[30] W. Brenig, Phys. Rev. B **56**, 2551 (1997).

[31] D. J. Lockwood, in *Light Scattering in Solids III*, Vol. 51 of *Topics in Applied Physics*, edited by M. Cardona and G. Güntherodt (Springer Verlag, Berlin, 1982), p. 59, and references therein.

[32] O. V. Misochko and E. Ya. Sherman, Physica C **222**, 219 (1994).

[33] P. Lemmens, M. Fischer, G. Els, G. Güntherodt, A. S. Mishchenko, M. Weiden, R. Hauptmann, C. Geibel, and F. Steglich, Phys. Rev. B **58**, 14 159 (1998).

[34] G. Bouzerar, A. P. Kampf, and G. I. Japaridze, Phys. Rev. B **58**, 3117 (1998).

[35] S. Schmidt, W. Palme, B. Lüthi, M. Weiden, R. Hauptmann, and C. Geibel, Phys. Rev. B **57**, 2687 (1998).

[36] H. Kuroe, H. Seto, J. Sasaki, T. Sekine, M. Isobe, and Y. Ueda, J. Phys. Soc. Jpn. **67**, 2881 (1998).

[37] M. Cottam and D. Lockwood, in *Light Scattering in Magnetic Solids* (Wiley, New York 1986), p. 135 ff.

[38] R. Merlin, G. Güntherodt, R. Humphreys, M. Cardona, R. Suryanarayanan, and F. Holtzberg, Phys. Rev. B **17**, 4951 (1978).

[39] J. Vitins, J. Magn. Magn. Mater. **5**, 212 (1977); J. Vitins and P. Wachter, Physica B **86-88**, 213 (1977).

[40] M. Isobe and Y. Ueda, J. Magn. Magn. Mater. **177-181**, 671 (1998).

[41] T. Ohama, H. Yasuoka, M. Isobe, and Y. Ueda, Phys. Rev. B **59**, 3299 (1999).

[42] M. Köppen, D. Pankert, R. Hauptmann, M. Lang, M. Weiden, C. Geibel, and F. Steglich, Phys. Rev. B **57**, 8466 (1998).

[43] P. Fertey, M. Poirier, M. Castonguay, J. Jegoudez, and A. Revcolevschi, Phys. Rev. B **57**, 13 698 (1998).

[44] This qualitative approach gives a big ratio $\Delta Q/\bar{Q}$. Typically, the phonon-induced charge transfer can be estimated as $\Delta Q/\bar{Q} \sim Cz_0/W$, where C is the electron phonon-coupling constant and $W\sim 1$ eV is the electron band width, respectively. Since a first-principle estimate gives $z_0\sim a(m/M)^{1/4}$ and $C\sim W/a$ (a is the lattice constant and m is the electron mass), $\Delta Q/\bar{Q} \sim(m/M)^{1/4}\sim 0.1$. However, in our case $W=2t_\perp$, that is rather small, while for the coupling we assume $C=eE_a$. The electric field of the oxygen ions surrounding V in the basal plane, diminishes the coupling. Note that not only the Coulomb forces but also the overlap of the oxygen and vanadium orbitals contribute to the value of C. Quantitatively, C can be determined only as a result of numerical band structure calculations. We suppose, however, that C is large enough since the asymmetry of the elementary cell is large.

[45] E. Ya. Sherman, Solid State Commun. **104**, 619 (1997).

[46] E. Ya. Sherman, M. Fischer, P. Lemmens, P. H. M. van Loosdrecht, and G. Güntherodt (unpublished).

[47] P. Wochner, J. M. Tranquada, D. J. Buttrey, and V. Sachan, Phys. Rev. B **57**, 1066 (1998).

[48] S.-H. Lee and S.-W. Cheong, Phys. Rev. Lett. **79**, 2514 (1997).